DOI: 10.1002/ejic.200500832

Density-Functional Calculation of the ^{183}W and ^{17}O NMR Chemical Shifts for Large Polyoxotungstates

Jose Gracia,[a] Josep M. Poblet,*[a] Jochen Autschbach,[c] and Leonid P. Kazansky*[b]

Keywords: Density-functional calculations / NMR spectroscopy / Tungsten / Oxygen / Polyoxometalates

A phosphane sulfate relativistic DFT method (ZORA) has been used to calculate the ^{183}W and ^{17}O NMR chemical shifts for large polyoxotungstates, including $W_6O_{19}^{2-}$, $CH_3OTiW_5O_{18}^{3-}$, $W_5O_{18}W^{II}NO^{3-}$, $W_{10}O_{32}^{4-}$, α-δ-γ-$XW_{12}O_{40}^{n-}$, β-$PW_9O_{28}Br_6^{3-}$, $P_2W_{18}O_{62}^{6-}$, $PW_2O_{14}^{3-}$, and $W_7O_{24}^{6-}$, based on their optimized molecular structures. Despite sizeable deviations between the calculated and experimental values, the calculations correctly reproduce the trends in the change of the chemical shift for both nuclei. As expected, the diamagnetic term is almost constant throughout the whole series. The change in the chemical shifts is shown to be determined by the paramagnetic term, which depends on the electronic structure of the whole anion under study and, in particular, on the local geometry around a given tungsten atom. On the other hand, there is no correlation between the chemical shift and HOMO–LUMO gap, showing that deeper occupied levels and several unoccupied orbitals play an important role in the paramagnetic term. However, analysis of the components of the paramagnetic shielding has shown that the most significant transitions determining the change of both ^{183}W and ^{17}O NMR chemical shifts for anions consisting of tungsten and oxygen atoms are the occupied–occupied and not the occupied–virtual ones.

Introduction

NMR spectroscopy is one of the powerful techniques for studying the problems of the chemistry of polyoxometalates (POM) formed by V, Mo, W, and other metals in high oxidation states[1] as it can be used to characterize them both in solution and in the solid state. POMs are usually built of metal–oxygen octahedra that form $M_nO_m^{z-}$ isopolyanions or $XM_nO_m^{z-}$ heteropolyanions. In many cases all nuclei can be observed in the NMR spectra, which helps to elucidate the chemical environment of the nucleus under study.

Several resonance lines may be observed in the NMR spectra depending on the complexity of an anion and its symmetry, and assigning each line to a particular atom sometimes presents a problem. The nature of the chemical shifts is therefore still to be revealed.

As a matter of fact there have been several attempts to understand the nature of the chemical shifts for POMs, and particularly for polyoxotungstates (POTs). The first such study attempted to explain the trend in the change of the ^{183}W NMR chemical shifts in lacunary POTs by the charge delocalization resulting from the removal of one W=O group from the Keggin anion $X^{x+}W_{12}O_{40}^{x-8}$.[2] Further, there have also been attempts to correlate the ^{17}O and ^{183}W chemical shifts with the wavelength of the lowest charge-transfer (LCT) band (the electronic transition from the MO localized mainly on the oxygen atoms to a virtual MO localized mainly on the metals),[3,4] with bond lengths,[5,6] with the inverse sum of the energy separations,[7,8] and with the calculated charges on atoms[9] obtained from EHMO calculations. However, the calculation of the actual chemical shielding for different nuclei is still to be attained.

The first attempts to calculate ^{183}W NMR chemical shifts were limited to small and simple molecules like $WO_{4-x}S_x^{2-}$, $W(CO)_6$, WF_6, and WCl_6, and a practically linear correlation between calculated and experimental shifts was found.[10,11] Calculation of the ^{17}O NMR chemical shifts in metal oxide anions MO_4^{n-} has been carried out by different methods with different degrees of accuracy.[12,13]

The first calculation of the ^{183}W chemical shift in a large Keggin anion using DFT was not so successful, and large discrepancies have been found by Bagno and co-workers even for small molecules.[14] Later, more reasonable calculated values of the ^{183}W NMR chemical shifts were obtained by the same authors.[15] A number of reviews of theoretical calculations of NMR chemical shifts in transition metal compounds have been published, including the results of ^{183}W chemical shift calculations by first-principles meth-

[a] Departament de Quimica Fisica i Inorgánica, Universitat Rovira i Virgili,
Pc. Imperial Tarraco 1, 43005 Tarragona, Spain
E-mail: josepmaria.poblet@urv.net
[b] Institute of Physical Chemistry, Russian Academy of Sciences, 31, Leninski pr, Moscow 119991, Russia
E-mail: leoka@ipc.rssi.ru
[c] Department of Chemistry, State University of New York at Buffalo,
312 Natural Sciences Complex, Buffalo, NY 14260-3000, USA
Supporting information for this article is available on the WWW under http://www.eurjic.org or from the author.

ods (relativistic Hartree–Fock and DFT).[16] However, those previous calculations were limited to comparatively small systems and no exhaustive theoretical study of chemical shifts in large heavy-metal POMs has yet been reported.

In the present work we have calculated the ^{183}W and ^{17}O nuclear magnetic shielding for several POTs using DFT methods with the goal of elucidating the relationship between the shielding and the geometric characteristics as well

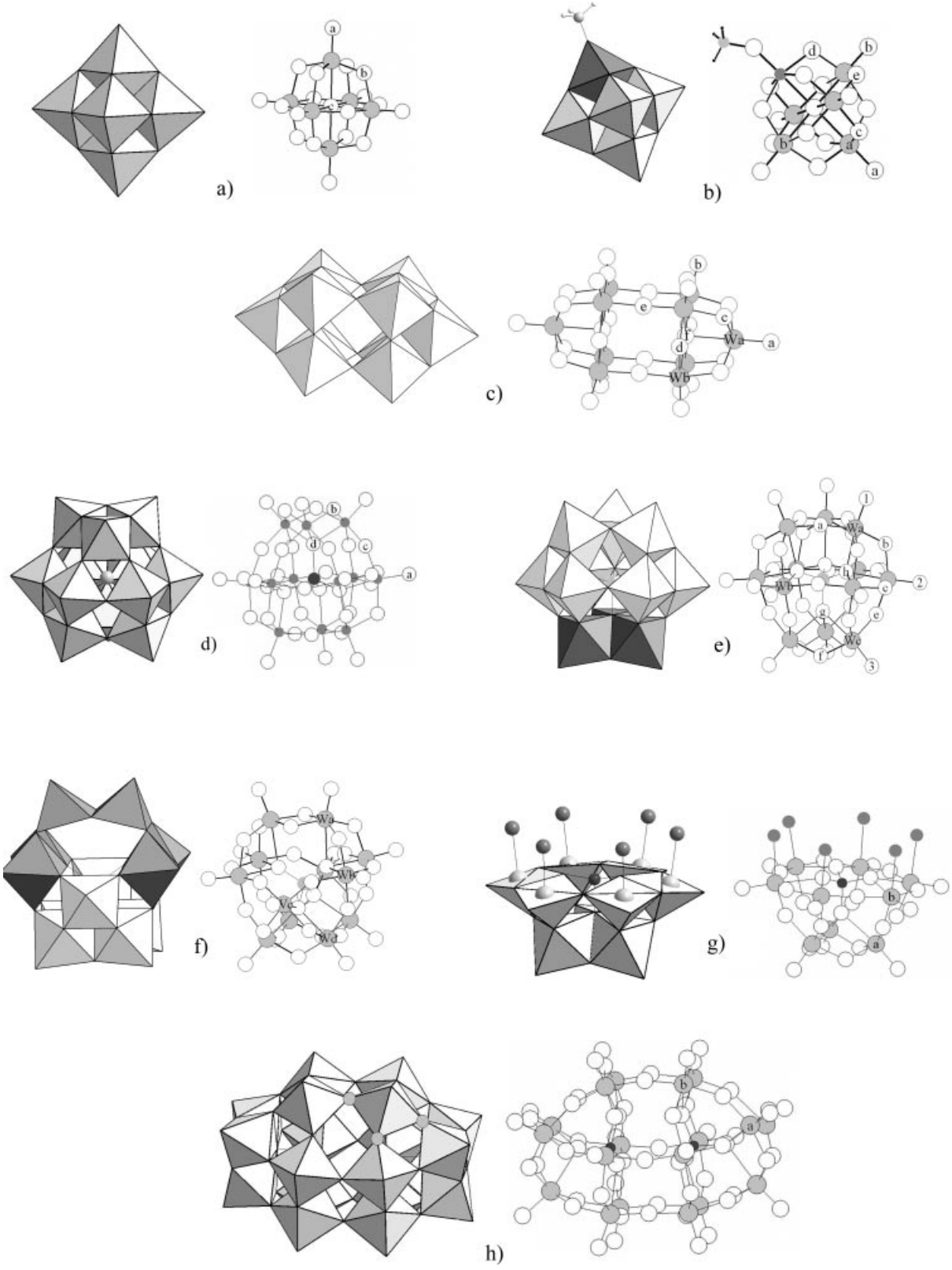

Figure 1. Polyhedral and ball-and-stick models for $W_6O_{19}^{2-}$ (a), $CH_3OTiW_5O_{18}^{3-}$ (b), $W_{10}O_{32}^{4-}$ (c), α-$XW_{12}O_{40}^{n-}$ (d), β-$SiW_{12}O_{40}^{4-}$ (e), γ-$SiW_{12}O_{40}^{4-}$ (f), β-$PW_9O_{28}Br_6^{3-}$ (g), and $P_2W_{18}O_{62}^{6-}$ (h).

as the influence of the latter on the chemical shifts. DFT methods have been shown to be adequate to rationalize many different aspects of the electronic structure,[17,18] magnetism,[19] and bonding[20] in POMs, and a summary of the most illustrative results can be found in a recent review.[21]

The first part of this study discusses several types of POTs (represented in Figures 1 and 2), namely the Lindqvist anion $W_6O_{19}^{2-}$ and its derivatives $CH_3OTiW_5O_{18}^{3-}$, $W_5O_{18}W^{II}NO^{3-}$, and $W_{10}O_{32}^{4-}$ (structural type I, characterized by edge sharing of WO_6 octahedra having a symmetry close to C_{4v}), the Keggin anions of general formula $XW_{12}O_{40}^{n-}$, their β and γ forms, and a bromide derivative (structural type II, with octahedra having two edge- and two corner-shared oxygen atoms), and the Dawson anion $P_2W_{18}O_{62}^{6-}$ (structural type III, where W_bO_6 octahedra have three corner-shared oxygen atoms). The octahedra in all these anions may be assigned as having local axial symmetry close to C_{4v}, with one terminal W=O bond. Finally,

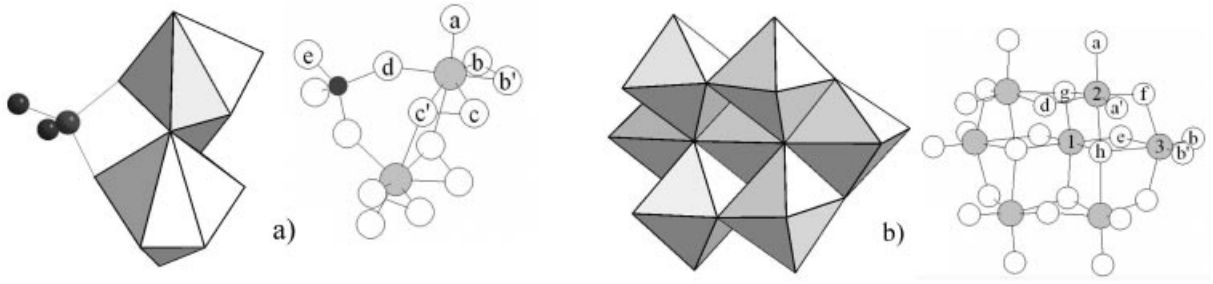

Figure 2. Polyhedral and ball-and-stick models for $PW_2O_{14}^{3-}$ (a) and $W_7O_{24}^{6-}$ (b).

Table 1. Experimental and calculated ^{183}W NMR shifts for several polyoxotungstates (POTs).

Anion type	Anion	W type	σ_p [ppm]	σ_d [ppm]	σ_t [ppm]	δ_{cal} [ppm]	δ_{exp} [ppm]	Ref. NMR	Ref. Struct.
0	WO_4^{2-}		–7002	9664	2663	0	0		
I	$W_6O_{19}^{2-}$		–7091	9658	2567	96	59	[2]	[28]
	$CH_3OTiW_5O_{18}^{3-}$	W_a	–7115	9658	2543	120	70	[29a]	[29a]
		W_b[a]	–7051	9659	2608	55	37		
	$W_5O_{18}W^{II}NO^{3-}$[b]	W_a^{VI}	–7183	9659	2476	187	117	[29b]	[29b]
		W_b^{VI}	–7221	9659	2438	225	168		
	$W_{10}O_{32}^{4-}$	W_a	–6841	9659	2818	–155	–166	[30]	[31]
		W_b	–6954	9658	2704	–41	–23		
II	$AsW_{12}O_{40}^{3-}$		–6897	9658	2761	–98	–65	[32]	[2,4]
	$GaW_{12}O_{40}^{5-}$		–6931	9657	2726	–63	–89		
	$GeW_{12}O_{40}^{4-}$		–6888	9657	2769	–106	–82		
	$PW_{12}O_{40}^{3-}$		–6842	9657	2815	–152	–99		
	$SiW_{12}O_{40}^{4-}$		–6864	9657	2793	–130	–104		
	$AlW_{12}O_{40}^{3-}$		–6897	9657	2760	–97	–113		
	$BW_{12}O_{40}^{5-}$		–6854	9657	2803	–140	–131		
	β-$SiW_{12}O_{40}^{4-}$	W_a	–6828	9657	2829	–166	–130	[33]	[2,34]
		W_b	–6833	9657	2824	–161	–115		
		W_c	–6871	9657	2786	–123	–110		
	γ-$SiW_{12}O_{40}^{4-}$	W_a	–6825	9658	2833	–170	–160	[35]	[36]
		W_b	–6864	9657	2793	–130	–105		
		W_c	–6810	9657	2847	–184	–117		
		W_d	–6836	9657	2821	–158	–127		
	β-$PW_9O_{32}B_6^{3-}$	W_a	–6846	9658	2812	–149	–123	[37]	[37]
		W_b	–7107	9658	2552	111	192		
III	$P_2W_{18}O_{62}^{6-}$	W_a	–6848	9657	2809	–146	–123	[38]	[39]
		W_b	–6779	9657	2878	–215	–174		
IV	$PW_2O_{14}^{3-}$		–6176	9659	3483	–820	–676	[40]	[40]
V	$W_7O_{24}^{6-}$	W_1	–7276	9658	2382	281	268	[41]	[42]
		W_2	–7024	9660	2636	27	–106		
		W_3	–6932	9662	2730	–67	–189		

[a] Average value for four slightly different W_b atoms due to bent $TiOCH_3$ group. [b] one W^{VI}=O group in $W_6O_{19}^{2-}$ is replaced by W^{II}-NO and the calculated shifts are given only for W^{VI} (apical and belt) as for $CH_3OTiW_5O_{18}^{3-}$.

the peroxo complex $PW_2O_{14}^{3-}$ (structural type IV) represents a POT where the tungsten has a formal coordination number of 7, with the lowest chemical shift, and the heptatungstate $W_7O_{24}^{6-}$ (structural type V) has three types of W, each of which has two terminal oxygen atoms.

The second part of the study will describe the results of the DFT calculations of the ^{183}W and ^{17}O chemical shifts for the corresponding reduced polyoxotungstates with delocalized, unevenly delocalized, and localized electrons.

Calculation of the Chemical Shielding

We used the ADF 2003.01 package[22] to compute the geometries of the molecules. The DFT calculations are characterized by the local density approximation featuring the *Xα* model for exchange with Becke's gradient-corrected functional,[23] and the VWN parameterization for correlation[24] corrected with Perdew's functional.[25] The basis functions for describing the valence electrons of all the atoms are Slater-type orbitals of triple-ζ+ polarization quality. The internal or core electrons are described by a relativistic core potential generated with the auxiliary program DIRAC.[22] The valence orbitals in this approach are kept orthogonal to the core orbitals by means of a single-ζ Slater-type core-orthogonalization basis set. We applied quasi-relativistic corrections to the valence shell by means of the zeroth-order relativistic approximation (ZORA). The NMR shielding tensors were computed from a parallel version of the NMR module.[26a] Although some previous studies have shown that all-electron basis sets reproduce the chemical shifts in some transition metal oxides better,[26b] we found no improvement in our results when this type of basis set was used for large POTs.

Generally, the W–O bonds in the optimized configurations are slightly longer than those observed in the X-ray structure determinations of the corresponding POTs. However, if we take the same anion but in different X-ray structures we sometimes see large discrepancies in the bond lengths. Even in a single crystal there may be two slightly different configurations with the same overall symmetry. Optimizing a structure results in a unique configuration for the given POT because, despite possible different initial coordinates, the program will end up delivering unique atomic coordinates, and although this may lead to an overestimation or underestimation of the calculated chemical shifts, such an approach is justified for comparison of the chemical shifts for different POTs, especially when accurate X-ray-determined coordinates are not available.

As usual, the calculated chemical shift, δ_{cal}, is determined as the difference between the total shielding of the reference molecule, σ_r, and the shielding of the molecule under study, σ_x. For each nucleus the total shielding tensor, σ_t, is calculated as the sum of the paramagnetic (σ_p) and diamagnetic (σ_d) contributions and therefore:

$$\delta_{cal} = \sigma_r - \sigma_x$$

where σ_x is the isotropic average of the shielding tensor for the nucleus in an anion and σ_r is the shielding of the reference compound.

The simplest oxoanion, WO_4^{2-}, is usually used as a reference for ^{183}W NMR chemical shifts and the resonance line of water is used as a reference for ^{17}O NMR chemical shifts. For convenience, the absolute shielding of liquid water, σ_t, is accepted to be equal to +291 ppm.[27]

The experimental values of ^{183}W chemical shifts may vary slightly depending on the spectrometer (sometimes by up to 10 ppm, and the chemical shifts of POTs are usually more positive in organic media. On the contrary, protonation of POT generally results in a negative shift of the resonance. Moreover, it should be noted that solvation effects are not included in these theoretical studies even though they can considerably influence the calculated chemical shift, which is assumed to refer to the gaseous state of a single molecule. Hence, we can only estimate a general trend in the chemical shifts from these calculations and, at best, to make an assignment of the resonances for a complex anion with nonequivalent nuclei.

Results

The ^{183}W NMR Chemical Shift

Table 1 gives the calculated paramagnetic, diamagnetic, and total shielding along with calculated and experimental ^{183}W NMR shifts for the POTs shown in Figures 1 and 2. (Table S1 in the Supporting Information shows the difference in the calculated parameters for the experimental and optimized structures of $W_6O_{19}^{2-}$ as an example).

It can be seen that the chemical shift decreases as the number of corner-sharing oxygen atoms increases (structures I→II→III) and that the most positive shift for W^1 in $W_7O_{24}^{4-}$, which formally has no terminal oxygen atoms, and the most negative shift for $PW_2O_{14}^{3-}$ are correctly predicted by the calculations. For the bromide derivative, the resonance assigned to the six W_b tungstens linked to bromide, observed at δ = +192 ppm, and the other line corresponding to W_a, observed at δ = –123 ppm, are also correctly predicted by the calculations. As expected, a soft ligand induces a large positive shift for the corresponding tungsten.

The order of the computed resonances corresponds to the observed one for both β-$SiW_{12}O_{40}^{4-}$ and for γ-$SiW_{12}O_{40}^{4-}$, and only the shift of W_c is rather exaggerated, probably due to an inadequate geometry.

In general, for anions consisting of WO_6 octahedra with an axial symmetry and a single W=O bond, including the peroxo anion, we observe a nice linear correlation between the calculated and experimental shifts for the POTs studied (Figure 3). The most notable deviations from this linear trend are observed for anions with the Keggin structure, which was shown by a more detailed analysis to be due to the structure-optimization process (as will be presented elsewhere). Briefly, the results of the latter depend strongly on the overall anionic charge, although for anions with the same negative charge, for example $XW_{12}O_{40}^{5-}$ (X = B^{III}, Al^{III}, and Ga^{III}), the observed and calculated shifts increase regularly with an increase of the inner tetrahedron.

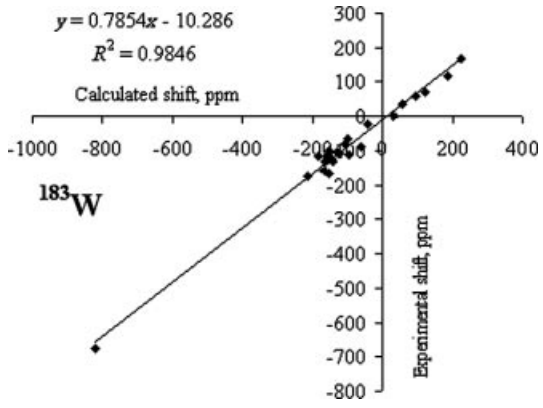

Figure 3. Correlation of the experimental and calculated ^{183}W NMR chemical shifts.

The ^{17}O NMR Chemical Shift

The ^{17}O NMR shifts depend strongly on the type of bonding (terminal or bridging) and the calculated values follow the experimental trend well (Table 2). A comparison of the calculated and experimental chemical shifts shows that the magnitude of the calculated shifts is overestimated for the bridging oxygen atoms and slightly underestimated for the terminal ones (Figure 4).

In the cases where the POT contains equal numbers of slightly different bridging oxygen atoms it is impossible to assign closely spaced resonances unequivocally in the experimental spectra. However, according to the calculations, the larger chemical shift for $CH_3OTiW_5O_{18}^{3-}$ (δ = 390 ppm) can be assigned to the bridging oxygen, O_c, linking two different tungsten atoms, and that at δ = 380 ppm to O_e (Table 2).

In the case of $W_{10}O_{32}^{4-}$, according to the calculations the two resonances at δ = 434 and 421 ppm observed in the experimental NMR spectrum should be attributed to the bridging oxygen, O_c, which links W_a and W_b and O_d, which is bound to two identical W_b lying in a square plane. For the oxygen atoms (O_e) in the linear bridges the calculated shift is the lowest, although it is observed between O_c and O_d in the experimental spectrum.

The bridging oxygen atoms in the Keggin anions $XW_{12}O_{40}^{n-}$ give two closely spaced resonances with equal intensity in the range δ = 440–390 ppm. Using a special method, which involves replacing three tungstens by molybdenum atoms, Shum and Klemperer[43b] have shown that the line with the larger chemical shift is due to the edge-sharing oxygens (O_b). According to the DFT calculations, the resonance with the larger chemical shift should be assigned to the edge bridging oxygen atoms O_b, which fully confirms the conclusions drawn from the experiment.

The rotation of a triplet in β-$SiW_{12}O_{40}^{4-}$ should formally result in the inequivalence of the oxygen atoms, with a corresponding weight ratio (according to the atom labels) of 3:6:3 for the terminal oxygen atoms and 3:6:3:3:6:3 for the bridging ones. However, only four lines are observed in the ^{17}O NMR spectrum, which were assigned[43b] as follows: the highest chemical shift was assigned to the terminal oxygen atoms, the line with intensity 3 to the edge-bridging O_c in the six-membered ring, the line with intensity 9 to the edge-bridging O_b and O_f, the line with intensity 12 to the corner bridging O_a, O_d, and O_e, and, finally, the less-intense line was assigned to the internal oxygens O_g and O_h. Our

Table 2. Calculated shielding and shifts and experimental ^{17}O shifts for several POTs.

Type	R_{W-O} [Å]	σ_p [ppm]	σ_d [ppm]	σ_t [ppm]	δ_{cal} [ppm]	δ_{exp} [ppm]	Ref.
$W_6O_{19}^{2-}$							
O_a	1.73	1.730	–880	401	770	775	[43]
O_b	1.953	1.953	–596	413	474	416	
O_c	2.357	2.357	–91	410	–28	–80	
$CH_3OTiW_5O_{18}^{3-}$							
O_b	1.75	–823	404	–419	710	721	[29]
O_a	1.75	–819	403	–416	707	713	
O_d	1.885	–703	416	–287	578	525	
O_c	1.938	–577	415	–162	453	390	
O_e	1.956	–570	414	–155	446	380	
O_f	2.361	–114	408	294	–3	–58	
$W_{10}O_{32}^{4-}$							
O_b	1.739	–863	403	–460	751	765	[31]
O_a	1.756	–820	404	–416	707	732	
O_c	1.953[a]	–621	418	–203	494	434	
O_e	1.923	–601	421	–180	471	423	
O_d	1.942	–609	415	–194	485	421	
O_f	2.341[a]	–162	404	242	–49	–2	
$PW_{12}O_{40}^{3-}$							
O_a	1.726	–873	401	–472	763	769	[43]
O_b	1.938	–619	419	–200	491	431	
O_c	1.93	–581	417	–164	455	404	
O_d	2.469	–218	398	180	111	70–60	
$SiW_{12}O_{40}^{4-}$							
O_a	1.737	–866	403	–463	754	761	[43]
O_b	1.943	–620	419	–201	492	427	
O_c	1.935	–584	418	–166	457	405	
O_d	2.38	–176	400	224	67	27	
β-$SiW_{12}O_{40}^{4-}$							
O_1	1.735	–864	403	–461	742[a]	762	[43b]
O_2	1.737	–861	403	–458			
O_3	1.735	–858	403	–455			
O_c	1.937	–650	420	–230	521	454	
O_b	1.946[a]	–614	419	–195	485[a]	425	
O_f	1.949	–612	419	193			
O_a	1.934	–588	419	–169	460[a]	404	
O_d	1.927	–584	419	–166			
O_e	1.941[a]	–589	418	–171			
O_g	2.390	–183	400	217	84[a]	32	
O_h	2.392	–179	397	218			
$W_7O_{24}^{6-}$							
O_a	1.781	–765	407	–358	663[a]	648	[41]
$O_{a'}$	1.772	–792	405	–387			
O_b	1.795	–686	407	–279	570	590	
$O_{b'}$	1.777	–747	406	–341	632	597	
O_e	1.796	–752	407	–345	636	626	
O_d	1.968	–545	413	–132	423	319	
O_f	1.973[a]	–507	411	–96	387	298	
O_g	2.049[a]	–455	410	–45	336	259	
O_h	2.260[a]	–286	407	121	170	74	

[a] Average value.

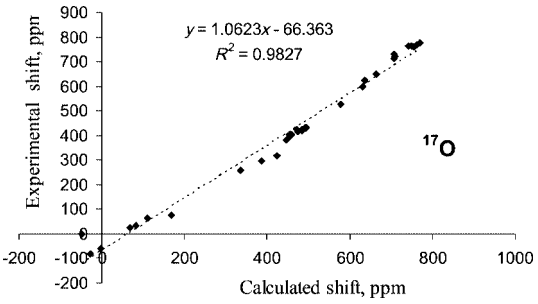

Figure 4. Correlation of the experimental and calculated ^{17}O NMR chemical shifts.

calculations fully confirmed the observed pattern, with the largest chemical shift for the bridging oxygen atoms O_c in the ring.

For $W_7O_{24}^{4-}$ the range of the ^{17}O NMR chemical shifts is fairly well reproduced by the calculations; a possible assignment of the lines is given in Table 2.

In general, a rather good linear correlation between the calculated and experimental ^{17}O NMR chemical shifts for POTs may be seen in Figure 4.

General Results

Taking into account all the calculated values for both ^{183}W and ^{17}O NMR chemical shifts, we have obtained good correlations between calculated and experimental values even though the NMR spectra were measured in different solvents in some cases. This shows that calculations adequately reflect the changes in chemical shifts depending on the structure. The discrepancies observed in some cases may result from the inadequacy of the optimized geometry, and the deviation of the slope from unity may be due to the basis sets used in the calculations.

Discussion

According to the present calculations the diamagnetic shielding (Tables 1 and 2) for both ^{183}W and ^{17}O is essentially unaffected by the geometry (the chemical environment). This can be understood from the fact that the diamagnetic shielding contains the unperturbed, zero-order density. The largest contributions are due to the core shells at ^{183}W and ^{17}O nuclei. Such core shells should not change on going from one chemical environment to another and therefore yield constant diamagnetic shielding contributions that cancel out in relative chemical shifts. Thus, we will consider only the paramagnetic contribution. In the following sections we discuss the analysis of the paramagnetic shielding tensors in a gauge-including atomic orbitals (GIAO) basis where a gauge-origin independent division into a paramagnetic and a diamagnetic contribution can be achieved.[26c]

The ^{183}W Paramagnetic Shielding

The paramagnetic contribution is determined by the magnetically perturbed MOs,[10] while the most important one is considered to be due to the coupling of the occupied (Ψ_a) and virtual (Ψ_i) MOs under the applied magnetic field. The magnitude of the coupling coefficients, u_{ai}, are given as[10]

$$u_{ai} \approx -\frac{1}{2(\varepsilon_i^0 - \varepsilon_a^0)}\langle \Psi_i | M | \Psi_a \rangle$$

where ε_i^0 and ε_a^0 are the orbital energies of the virtual and occupied MOs. We will refer to the "u-tensor" in conjunction with nuclear shielding contributions arising from these coefficients and note that inverse occupied–virtual MO energy differences enter these terms. Thus, common knowledge often relates the magnitude of the paramagnetic shielding to the size of the HOMO–LUMO gap, for example.

The paramagnetic shielding is determined by the sum of all magnetically active transitions and by atomic orbital coefficients forming the corresponding MOs. For the large anions, which consist of tungsten and oxygen atoms, so many MOs are formed that it is rather difficult to show which transitions are the most important in the paramagnetic shielding. However, a preliminary analysis of the paramagnetic shielding for $W_6O_{19}^{2-}$ shows that the largest contributions (about 15%) come from two transitions from rather deep bonding MOs ($5t_{1g}$), involving p and d orbitals of the bridging oxygen and tungsten atoms, respectively, not to the LUMO but to upper virtual orbitals (a_{1g} and e_g), consisting of W-d_{z^2} and p- and s-oxygen orbitals. Moreover, terms involving pairs of occupied orbitals should be also taken into account. In the paramagnetic shielding, this is a term, from now on dubbed "*s*-tensor", that is specific to the computation of the nuclear shielding in a GIAO basis, where the external magnetic field will change the overlap between the basis functions (atomic orbitals or AOs). In the case of ^{183}W shielding it can attain 15% of the total paramagnetic term, which is mostly due to the occupied–virtual transitions ("*u*-tensor"). For the paramagnetic contribution of the terminal oxygen atom in the case of the Lindqvist anion, for example, 163 occupied–occupied ("*s*-tensor") and 238 occupied–virtual (*u*-tensor) couplings should be taken into account, and for the latter less than 50 transitions exceed 10 ppm. For the bridging oxygen the number of transitions increases to 488 and 744, respectively, and some transitions contribute with opposite signs.

Two points should be mentioned. First of all, the lowest charge transfer, determined as the HOMO–LUMO gap, E_{LCT}, is by no means the principal contributor otherwise we should observe a correspondence between $1/E_{LCT}$ and the ^{183}W chemical shifts (see Table S2 in the Supporting Information). Usually, the HOMO is a nonbonding orbital consisting of the p-orbitals of the bridging oxygen atoms, especially of the inner oxygen atoms, and even for simpler complexes the transitions from deeper MOs, involving several metallic orbitals, make the largest contributions.

As already mentioned, the paramagnetic shielding includes not only the *u*-term, which involves the occupied and virtual MO coupling and plays a dominant role in the

change of the chemical shift, but also the occupied–occupied MO coupling (*s*-tensor) and additional "paramagnetic gauge terms". The latter are also related to the GIAO formalism (they are negligibly small in the present study, see discussion on the components of the paramagnetic shielding[44] and Table 3). In frozen-core calculations there is, in addition, a frozen-core term (dubbed "*b*-tensor" here) that stems from the change of the valence-core orthogonalization under the external magnetic-field perturbations. As for POTs, the magnitudes of the changes in the *s*- and *b*-tensors may be comparable with the *u*-term and therefore they demand more consideration in detail:

Table 3. Parameters of the paramagnetic shielding (σ_p) of ^{183}W NMR for some POTs.[a]

Anion	Metal/X	*b*-term [ppm]	*s*-term [ppm]	*u*-term [ppm]	PGT [ppm]	R_{W-O} [Å]	δ_{cal} [ppm]
$W_{10}O_{32}^{4-}$	W_a	262	–730	–6384	11	1.966	–155
	W_b	358	–882	–6437	7	1.978	–41
$W_6O_{19}^{2-}$		358	–1002	–6454	7	1.983	96
$CH_3OTiW_5O_{18}^{3-}$	W_b	397	–1068	–6385	7	1.982	55
	W_a	366	–1014	–6474	7	1.983	120
$W_5O_{18}W(II)NO^{3-}$	W_a	321	–917	–6594	7	1.986	187
	W_b	359	–1015	–6571	6	1.991	225
$XW_{12}O_{40}^{n-8}$	As	140	–295	–6752	10	1.981	–98
	Ga	119	–212	–6759	9	1.989	–152
	Ge	242	–545	–6595	10	1.975	–106
	P	222	–470	–6625	9	1.979	–130
	Si	332	–791	–6482	10	1.966	–63
	Al	323	–746	–6483	9	1.972	–97
	B	228	–475	–6615	8	1.981	–140
β-$SiW_{12}O_{40}^{4-}$	W_a	192	–404	–6624	8	1.981	–166
	W_b	232	–499	–6575	9	1.976	–162
	W_c	204	–431	–6653	9	1.984	–123
γ-$SiW_{12}O_{40}^{4-}$	W_a	43	–2	–6873	7	2.017	–171
	W_b	237	–513	–6596	8	1.978	–130
	W_c	236	–521	–6535	10	1.973	–184
	W_d	201	–433	–6613	9	1.978	–158
β-$PW_9Br_6O_{28}^{3-}$	W_a	74	–90	–6836	6	1.987	–149
	W_b	125	–164	–7071	3	2.078	111
$X_2W_{18}O_{62}^{6-}$	W_b	127	–134	–6785	13	1.981	–215
	W_a	8	134	–6999	9	1.983	–146
$PW_2O_{14}^{3-}$		482	–533	–6119	–5	1.960	–820
$W_7O_{24}^{6-}$	W_1	585	–1525	–6344	8	2.024	283
	W_2	170	–399	–6797	2	1.964	47
	W_3	158	–372	–6720	2	1.972	–77

[a] B-tensor: direct frozen core terms (B1 tensor); S-tensor: OCC-OCC terms (paramagnetic SMAT1 tensor); U-tensor: OCC-VIR terms (paramagnetic UMAT1 tensor); PGT: DIAG. OCC-OCC terms (for gauge invariance, paramagnetic gauge tensor).

1. For anions with octahedra having only *edge-shared* oxygen atoms (the first four, Figures 1a–c) and the internal oxygen linking six and five tungsten atoms, for a span of the experimental shifts of 334 ppm (span of the calculated shifts: 380 ppm), increasing the mean R_{WO} results in a negative shift (–135 ppm) due to the *b*-term but in positive shifts due to the *s*-term (338 ppm) and the *u*-term (only 210 ppm). The total shift therefore increases with R_{WO}.
2. As opposed to the Lindqvist-type anions, α-Keggin anions (Figure 1d), with their narrow range (89 ppm) of calculated shifts (66 ppm for experimental ones), and with two corner and two edge-shared oxygen atoms and the inner oxygen linking three W atoms and the central atom, an increase of the mean R_{WO} in the optimized structures corresponds to a general decrease of the chemical shift due to a decrease in the *b*-term (213 ppm) and the *u*-term (277 ppm; both of which correspond to an increase in the chemical shift), which is outweighed by the negative shift due to the *s*-term (–579 ppm); a fine interplay of these components therefore determines the total chemical shift.

For the β-γ Keggin isomers and $P_2W_{18}O_{62}^{6-}$ a decrease of the *b*-term from 237 to 8 ppm (Δ = –229 ppm) and the *u*-term from –6534 to –6999 ppm (Δ = –465 ppm, for a total of –694 ppm) is close to the increase of the *s*-term from –521 to 134 ppm (Δ = 655 ppm).

The second point is that the absolute values of the *s*-term for the Lindqvist-type anions are almost twice as large as for the Keggin anions. On the other hand, the pentacoordination of W_a in γ-$SiW_{12}O_{40}^{4-}$ (Table 3, Figure 1e) results in a rather small magnitude of the *s*-term; this is probably characteristic for pentacoordination.

It is noteworthy that the *u*-term for W_a in $P_2W_{18}O_{62}^{6-}$ is the lowest of all WO_6 octahedra, which is difficult to explain as the local symmetry around W_a is almost the same as in the Keggin system. However, despite substantial differences in the components of the paramagnetic shielding, the calculated ^{183}W chemical shifts for the Keggin anion and for W_a of the Dawson anion proved to be almost the same, reflecting the similarity of the local geometry.

Some unusual values of the *b*- and *u*-terms for the Dawson anion may be explained by the correlations of the *b*- and *s*- against the *u*-term as the largest component (anions α-$XW_{12}O_{40}^{n-8}$, β-$SiW_{12}O_{40}^{4-}$, γ-$SiW_{12}O_{40}^{4-}$, $X_2W_{18}O_{62}^{6-}$) shown in Figure 5. It is clearly seen that three components are interrelated, but only for similar types of anions.

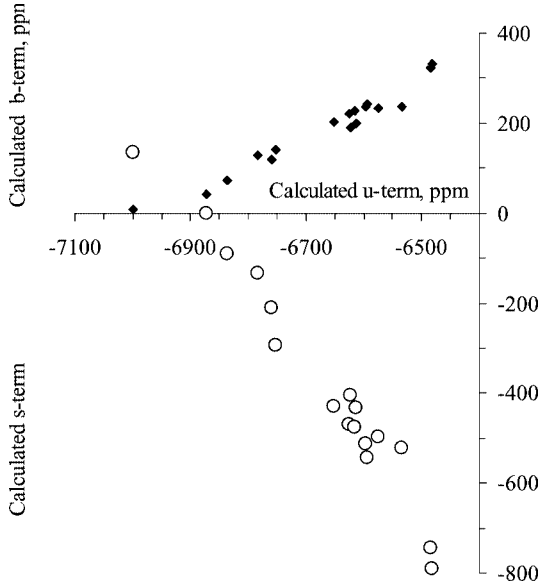

Figure 5. Interrelation between paramagnetic *u*- and *b*- (♦) and *s*- (○) terms for POTs (α-$XW_{12}O_{40}^{n-8}$, β-$SiW_{12}O_{40}^{4-}$, γ-$SiW_{12}O_{40}^{4-}$, $X_2W_{18}O_{62}^{6-}$).

In general, we can observe that increasing R_{WO} results in a corresponding absolute increase in the *u*-term (the more negative the shielding the more positive the chemical shift)

determined by the occupied–virtual MO transitions (see Figure S1 in the Supporting Information) That, in turn, depends on the bonding system (edge, corner, inner oxygen atoms, and angles between bonds) and determines the change of the *b* and *s* shielding components. In any case, the *s*-term changes in a broader range than the *u*-term, which is usually considered as the most important. For POTs, where tungsten is surrounded only by oxygen atoms as ligands, we can suggest that the change of the chemical shift is determined by the total paramagnetic contribution, in which the occupied–occupied transitions have proved to be the most important, and a fine interplay of the components (*s*- and *u*-terms) of the paramagnetic shielding variable in quite a large range will determine the total chemical shift. Nevertheless, the calculation adequately represents the general trend in the chemical shifts.

It should be noted that the *u*- and *s*-terms decrease with R_{WO} for the anions built with octahedra linked by edge-shared oxygens and therefore a close correlation between the experimental shifts and the sum of the inversed energies of the electronic transitions between d and d* orbitals calculated by the EHMO method is observed.[8]

The ^{17}O Paramagnetic Shielding

For the terminal oxygen atoms the *s*-term makes no more than 5% contribution to the paramagnetic *u*-term and the core *b*-term is much lower (Table 4). For the inner oxygen the *s*-term may reach 30% and moreover is of opposite sign, therefore it makes a sizeable contribution. Only for $W_6O_{19}^{2-}$ is the *s*-term for O_c negative as it binds six tungsten atoms. For $W_{10}O_{32}^{4-}$, where the inner oxygen atoms O_f bind five W atoms, and for O_d in the Keggin anion, which binds four atoms, the *s*-term becomes positive.

Table 4. Components of the ^{17}O paramagnetic shielding for some POTs.

Anion	Atom	*b*-term [ppm]	*s*-term [ppm]	*u*-term [ppm]	PGT [ppm]	R_{W-O} av. [Å]
$W_{10}O_{32}^{4-}$	O_a	1	–36	–787	1	1.756[a]
	O_c	–2	–9	–596	–15	1.938, 1.969[a]
	O_f	–7	114	–276	8	2.288, 2.354[a]
	O_b	0	7	–868	–2	1.739[b]
	O_d	–3	–7	–594	–5	1.942[b]
	O_e	–4	–82	–521	7	1.923[b]
$W_6O_{19}^{2-}$	O_a	1	–1	–880	0	1.730
	O_b	–2	–15	–573	–7	1.953
	O_c	–5	–26	–74	14	2.357
$PW_{12}O_{40}^{3-}$	O_a	1	34	–905	–3	1.726
	O_b	–2	–14	–593	–9	1.938
	O_c	–4	–23	–556	2	1.930
	O_d	–8	121	–355	23	2.469

[a] Distance to W_a. [b] Distance to W_b.

Depending on the type of oxygen atom (corner- or edge-shared), the absolute value of the *s* component is larger for the corner one. However, because the bond length in corner sharing is usually shorter than that for an edge-sharing oxygen, the absolute *u*-term is less, making more negative shift for the corner oxygen that links two equivalent tungsten atoms having the same chemical shift. If it binds two tungsten atoms with different chemical shifts (as O_c in $W_{10}O_{32}^{4-}$), the magnitude becomes unpredictable.

However, from Figure 6 (taking into account data for anions $W_6O_{19}^{2-}$, $W_{10}O_{32}^{4-}$, $CH_3OTiW_5O_{18}^{3-}$, α-$PW_{12}O_{40}^{3-}$, α-$SiW_{12}O_{40}^{4-}$, and β-$SiW_{12}O_{40}^{4-}$) the interrelation between the *u*-term and the *s*-term for three types of oxygen atoms − terminal, bridging, and inner − is clearly seen. A certain similarity between this plot and the one given in Figure 5 may be noted.

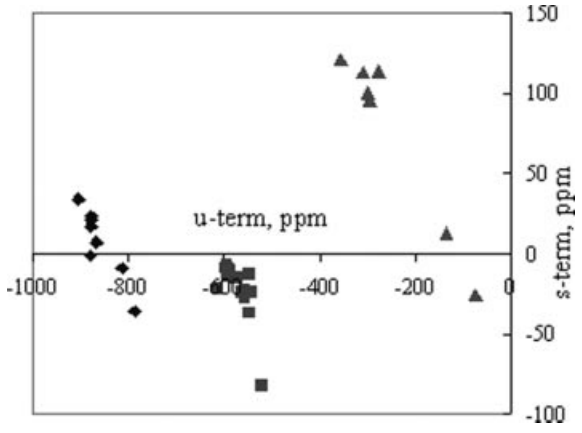

Figure 6. Interrelation of the *u*- and *s*-terms in the ^{17}O paramagnetic shielding for POT. ♦: terminal oxygen atoms; ■: bridging oxygen atoms; ▲: inner oxygen atoms.

For all POTs the most deshielded ones proved to be the terminal oxygen atoms. Although the shorter bond length leads to increased ΔE, it is possible that an increase of the numerator exceeds the effect of decreasing $1/\Delta E$ (see formula above).

Conclusions

Having considered the results of calculations of the ^{183}W and ^{17}O NMR chemical shifts we can come to the following conclusions: 1) Generally, the calculations reproduce the patterns of the chemical shifts for both nuclei for several types of tungsten and oxygen atoms. However, when the range of the chemical shifts is rather narrow, prediction of the chemical shifts will depend on the chosen geometric parameters, and a fine interplay of the different components of the paramagnetic shielding may result in discrepancies between the calculated and experimental chemical shifts, as, for example, for γ-$SiW_{12}O_{40}^{4-}$. 2) The accuracy of the calculated chemical shifts is far from what would be desirable and, in principle, a complete compatibility between calculated and observed chemical shifts is still not possible for such polyoxotungstate complexes because of inaccuracies in the geometric characteristics obtained by X-ray diffraction studies. Sometimes, even for rather simple peroxotungstates with overall C_2 symmetry, two tungstens are crystallographically not identical and their different local geometry may

easily give rise to differences of 200 ppm or more in the calculated chemical shifts. Therefore, for sake of consistency, the optimized structures, despite some inadequacy, may be an adequate approach for the calculation of the NMR shielding. 3) For POTs consisting of tungsten and oxygen atoms the change in the chemical shifts is determined by an interplay of the components of the paramagnetic shielding, in which the main contributor has been shown to be the *s*-term (the occupied–occupied MO coupling) along with the change in the *u*-term (the occupied–virtual MO transitions). Apparently, such a behavior of the paramagnetic shielding is characteristic, as shown by our preliminary results, for other polyoxometalates involving vanadium or molybdenum. 4) From the accumulated data the reverse task may, in principle, become possible, namely deducing the geometry from the observed chemical shifts, if the nature of the nuclear shielding is completely understood. 5) At present, the reliable assignment of the several resonance lines observed in the NMR spectra to specific atoms may be made only in the case of widely separated NMR shifts. The fine details of the anion geometry must therefore be taken into account to be able to assign the resonances correctly. 6) It is rather well known[10,11,45] that taking into account the spin-orbit coupling during calculation of the chemical shift of heavy elements notably increases the correspondence between the calculated and experimental shifts. This is especially true when the ligands around the coordinating cation are quite different and heavy. However, although our preliminary calculations for POTs where the ligand atoms are only oxygen atoms, obtained by including the SO coupling term, give slightly more reasonable values in terms of magnitude, they do not give the correct order of the resonances for the Keggin anions and even violate the sequence of the lines for β- and γ-$SiW_{12}O_{40}^{4-}$.

Thus, to improve the accuracy of computed NMR chemical shifts in polyoxometalates is not simple and will require effort in several areas, most notably to incorporate exact exchange functionals in the DFT calculations, to consider the spin-orbit coupling, and to use larger basis sets. The reader must bear in mind that the calculation of the shielding tensors for *one* atom of the Dawson anion $P_2W_{18}O_{62}^{6-}$ needs more than ten days of computer time.[46] Therefore, it will be necessary to further improve the codes of NMR calculations for large systems, and probably for clusters with relatively large *q*/*m*, where *q* is charge and *m* the number of metals, to introduce the effect of the solvent.[47]

Supporting Information (see also footnote on the first page of this article): Influence of the geometric parameters on calculated shieldings for $W_6O_{19}^{2-}$ and HOMO–LUMO separation for several POTs are given in Tables S1 and S2. The correlation between calculated paramagnetic shielding and mean bond length, R_{W-O}, in Keggin anions is given in Figure S1.

Acknowledgments

This work was supported by the Spanish MECD (BQU2002-04110-C02-01) and the CIRIT of the Autonomous Government of Catalonia (SGR01-00315). J.A. is grateful for financial support from the CAREER program of the National Science Foundation (grant no. CHE-0447321). The authors thank the referees for comments and suggestions.

[1] a) *Chem. Rev.* **1988**, *98*, special issue, Ed.: C. Hill; b) *Polyoxometalate-Molecular Science* (Eds.: J. J. Borrás-Almenar, E. Coronado, A. Müller, M. T. Pope). NATO Science Series, II. Mathematics, Physics and Chemistry, vol. 98, Kluwer Academic Publishers, Dordrecht, The Netherlands, **2003**.
[2] O. A. Gansow, R. K. C. Ho, W. G. Klemperer, *J. Organomet. Chem.* **1980**, *187*, 27.
[3] L. P. Kazansky, *Koord. Khim.* **1977**, *3*, 327.
[4] R. Acerete, C. F. Hammer, L. C. W. Baker, *J. Am. Chem. Soc.* **1982**, *104*, 5384.
[5] L. P. Kazansky, M. A. Fedotov, V. I. Spitsyn, *Doklady Akad. Nauk SSSR* **1983**, *272*, 1179.
[6] L. P. Kazansky, *Chem. Phys. Lett.* **1994**, *223*, 289.
[7] L. P. Kazansky, P. Chaquin, M. Fournier, G. Herve, *Polyhedron* **1998**, *17*, 4353.
[8] M. Inoue, T. Yamase, L. P. Kazansky, *Polyhedron* **2003**, *22*, 1183.
[9] L. P. Kazansky, T. Yamase, *J. Phys. Chem. A* **2004**, *108*, 6437.
[10] A. Rodrigues-Fortea, P. Alemany, T. Ziegler, *J. Phys. Chem. A* **1999**, *103*, 8288.
[11] M. Hada, H. Kaneko, H. Nakatsuji, *Chem. Phys. Lett.* **1996**, *261*, 7.
[12] M. Kaupp, O. L. Malkina, V. G. Malkin, *J. Chem. Phys.* **1997**, *106*, 9201.
[13] G. Schreckenbach, T. Ziegler, *Int. J. Quantum Chem.* **1997**, *61*, 899.
[14] A. Bagno, M. Bonchio, *Chem. Phys. Lett.* **2000**, *317*, 12.
[15] A. Bagno, M. Bonchio, A. Sartorel, G. Scorrano, *ChemPhysChem.* **2003**, *4*, 4353.
[16] a) J. Autschbach, *The Calculation of NMR Parameters in Transition Metal Complexes*, in *Density Functional Theory in Inorganic Chemistry*, Vol. 112 (Eds.: N. Kaltsoyannis, J. E. McGrady), Springer, Heidelberg, **2004**; b) J. Autschbach, *Calculation of Heavy-Nucleus Chemical Shifts: Relativistic All-Electron Methods*, in *Calculation of NMR and EPR Parameters. Theory and Applications* (Eds.: M. Kaupp, M. Bühl, V. G. Malkin), Wiley-VCH, Weinheim, **2004**. See also c) M. Kaupp, V. G. Malkin, O. L. Malkina, *NMR of Transition Metal Compounds*, in *Encyclopedia of Computational Chemistry* (Ed.: P. v. R. Schleyer), John Wiley & Sons, Chichester, **1998**, pp 1857–1866; d) M. Bühl, M. Kaupp, M. O. L. Malkina, V. G. Malkin, *J. Comput. Chem.* **1999**, *20*, 91–105.
[17] M.-M. Rohmer, M. Bénard, E. Cadot, F. Sécheresse, *Polyoxometalate Chemistry: From Topology via Self-Assembly to Applications* (Eds.: M. T. Pope, A. Müller), Kluwer Academic, Dordrecht, The Netherlands, **2001**, p. 117; M.-M. Rohmer, M. Bénard, *Chem. Soc. Rev.* **2001**, *30*, 340.
[18] J. M. Maestre, X. López, C. Bo, J. M. Poblet, N. Casañ-Pastor, *J. Am. Chem. Soc.* **2001**, *123*, 3749; X. López, J. M. Maestre, C. Bo, J. M. Poblet, *J. Am. Chem. Soc.* **2001**, *123*, 9571; C. X. López, J. M. Poblet, *J. Am. Chem. Soc.* **2002**, *124*, 12574.
[19] S. A. Borshch, *Inorg. Chem.* **1998**, *37*, 3116; H. H. Duclusaud, S. A. Borshch, *J. Am. Chem. Soc.* **2001**, *123*, 2825; S. A. Borshch, H. Duclusaud, J. M. Millet, *Appl. Cat. A: General* **2000**, *200*, 103.
[20] A. Bridgeman, *Chem. Phys.* **2003**, *287*, 55; A. Bridgeman, G. Cavigliasso, *Chem. Phys.* **2002**, *279*, 143; A. Bridgeman, G. Cavigliasso, *J. Phys. Chem. A* **2003**, *107*, 6613.
[21] J. M. Poblet, X. López, C. Bo, *Chem. Soc. Rev.* **2003**, *32*, 297.
[22] ADF 2003.1; Department of Theoretical Chemistry, Vrije Universiteit, Amsterdam, J. Baerends; D. E. Ellis, P. Ros, *Chem. Phys.* **1973**, *2*, 41; L. Versluis, T. Ziegler, *J. Chem. Phys.* **1988**, *88*, 322; G. Te Velde, E. J. Baerends, *J. Comput. Phys.* **1992**, *99*, 84; C. Fonseca Guerra, J. G. Snijders, G. Te Velde, E. J. Baerends, *Theor. Chem. Acc.* **1998**, *99*, 391.

[23] A. D. Becke, *J. Chem. Phys.* **1986**, *84*, 4524; A. D. Becke, *Phys. Rev.* **1988**, *A38*, 3098.
[24] S. H. Vosko, L. Wilk, M. Nusair, *Can. J. Phys.* **1980**, *58*, 1200.
[25] J. P. Perdew, *Phys. Rev. B* **1986**, *33*, 8822; J. P. Perdew, *Phys. Rev. B* **1986**, *34*, 7406.
[26] The parallelized spin-orbit version of the NMR code has been improved by J. A. in order to achieve more favorable scaling with increasing system size as compared to the original implementation: a) J. Autschbach, E. Zurek, *J. Phys. Chem. A* **2003**, *107*, 4967–4972; b) R. Bouten, E. J. Baerends, E. van Lenthe, L. Visscher, G. Schreckenbach, T. Ziegler, *J. Phys. Chem. A* **2000**, *104*, 5600; c) S. K. Wolff, T. Ziegler, E. van Lenthe, E. J. Baerends, *J. Chem. Phys.* **1999**, *110*, 7689; d) G. Schreckenbach, *Theor. Chem. Acc.* **2002**, *108*, 246.
[27] D. Sundholm, J. Gauss, A. Schäfer, *J. Chem. Phys.* **1996**, *105*, 11051.
[28] a) N. I. Krylov, I. S. Kolomnikov, *Koord. Khim.* **1977**, *3*, 1895; b) J. Fuchs, W. Freiwald, H. Hartl, *Acta Crystallogr., Sect. B* **1978**, *34*, 1764.
[29] a) W. Clegg, M. R. J. Elsegood, R. J. Errington, J. J. Havelock, *J. Chem. Soc., Dalton Trans.* **1996**, 681; b) A. Proust, R. Thouvenot, S. G. Roh, J. K. Yoo, P. Gouzerh, *Inorg. Chem.* **1995**, *34*, 4106–4112.
[30] a) J. Fuchs, H. Hartl, W. Schiller, U. Gerlach, *Acta Crystallogr., Sect. B* **1976**, *32*, 740; b) Y. Sasaki, T. Yamase, Y. Ohashi, Y. Sasada, *Bull. Chem. Soc. Jpn.* **1987**, *60*, 4285.
[31] a) L. P. Kazansky, M. A. Fedotov, V. I. Spitsyn, *Dokl. Acad. Nauk SSSR* **1983**, *272*, 1179; b) D. C. Duncan, C. L. Hill, *Inorg. Chem.* **1996**, *35*, 5828.
[32] G. M. Brown, M.-R. Noe-Spirlet, W. R. Busing, H. A. Levy, *Acta Crystallogr., Sect. B* **1977**, *33*, 1038.
[33] a) K. Y. Matsumoto, A. Kobayashi, Y. Sasaki, *Bull. Chem. Soc. Jpn.* **1975**, *48*, 3146; b) J. Fuchs, A. Thiele, Z. R. Palm, *Z. Naturforsch., Teil B* **1981**, *36*, 161–171; c) F. Robert, A. Tezé, G. Hervé, Y. Jeannin, *Acta Crystallogr., Sect. B* **1980**, *36*, 11.
[34] J. Lefebvre, F. Chauveau, P. Doppelt, C. Brevard, *J. Am. Chem. Soc.* **1981**, *103*, 4589.
[35] A. Tezé, E. Cadot, V. Béreau, G. Hervé, *Inorg. Chem.* **2001**, *40*, 2000.
[36] A. Tezé, J. Canny, L. Gurban, R. Thouvenot, G. Hervé, *Inorg. Chem.* **1996**, *35*, 1001.
[37] R. J. Errington, R. L. Wingad, W. Clegg, M. R. J. Elsegood, *Angew. Chem. Int. Ed.* **2000**, *39*, 3884.
[38] a) R. Acerete, C. F. Hammer, L. C. W. Baker, *Inorg. Chem.* **1984**, *23*, 1478; b) R. Acerete, C. F. Hammer, L. C. W. Baker, *Inorg. Chem.* **1984**, *23*, 1478.
[39] a) H. D'Amour, *Acta Crystallogr., Sect. B* **1976**, *32*, 729; b) V. S. Sergienko, M. A. Porai-Loshits, S. V. Kiselev, L. A. Butman, V. F. Chuvaev, *Z. Neorgan. Khim.* **1983**, *28*, 1199.
[40] L. Salles, C. Aubry, R. Thouvenot, F. Robert, C. Doremieux-Morin, G. Chottard, H. Ledon, Y. Jeannin, J.-M. Brégeault, *Inorg. Chem.* **1994**, *33*, 871.
[41] a) K. G. Burtseva, T. S. Chernaya, M. I. Sirota, *Doklady AN SSSR* **1978**, *243*, 104; b) J. Fuchs, E. P. Flint, *Z. Naturforsch., Teil B* **1979**, *34*, 412.
[42] a) R. I. Maksimovskaya, K. G. Burtseva, *Polyhedron* **1985**, *4*, 1559; b) J. J. Hastings, O. W. Howarth, *J. Chem. Soc., Dalton Trans.* **1992**, 209.
[43] a) C. J. Besecker, W. K. Klemperer, F. J. Maltbie, *Inorg. Chem.* **1985**, *24*, 1027; b) W. Shum, thesis; W. G. Klemperer, personal communication.
[44] G. Schreckenbach, T. Ziegler, *Int. J. Quantum Chem.* **1996**, *60*, 753.
[45] a) J. Autschbach, T. Ziegler, *Relativistic Computation of NMR Shieldings and Spin-Spin Coupling Constants*, in *Encyclopedia of Nuclear Magnetic Resonance*, Vol. 9 (Eds.: D. M. Grant, R. K. Harris), John Wiley & Sons, Chichester, **2002** (see also ref.[16]); b) M. Kaupp, O. L. Malkina, V. G. Malkin, P. Pyykkö, *Chem. Eur. J.* **1998**, *4*, 118–126; c) S. K. Wolff, T. Ziegler, *J. Chem. Phys.* **1998**, *109*, 895–905.
[46] Calculation running in parallel in a five Pentium 4 (2.5 GHz) cluster.
[47] X. López, J. A. Fernández, S. Romo, J. F. Paul, L. Kazansky, J. M. Poblet, *J. Comput. Chem.* **2004**, *25*, 1542.

Received: December 1, 2005
Published Online: February 6, 2006

